Journal of Hydrology: Regional Studies 32 (2020) 100739

Contents lists available at ScienceDirect

Journal of Hydrology: Regional Studies

journal homepage: www.elsevier.com/locate/ejrh

Bayesian estimates of the mean recharge elevations of water sources in the Central America region using stable water isotopes

L. Nicole Arellano [a,b,*], Stephen P. Good [a], Ricardo Sánchez-Murillo [c], W. Todd Jarvis [d], David C. Noone [e,f], Catherine E. Finkenbiner [a]

[a] Department of Biological and Ecological Engineering, Oregon State University, 116 Gilmore Hall, Corvallis, OR, 97331-8545, United States
[b] Department of Earth and Atmospheric Sciences, University of Houston, Science and Research Building 1 Room 214, 3507 Cullen Blvd, Houston, TX 77204-5008, United States
[c] Stable Isotopes Research Group and Water Resources Management Laboratory, Universidad Nacional, P.O. Box 86-3000, Heredia, Costa Rica
[d] Institute for Water and Watersheds, Oregon State University, 234 Strand Agricultural Hall, Corvallis, OR, 97331-2208, United States
[e] College of Earth, Ocean, and Atmospheric Sciences, Oregon State University, 104 CEOAS Administration Building, Corvallis, OR, 97331-5503, United States
[f] Department of Physics, University of Auckland, Science Centre - Building 303 Level 6, 38 Princes St, Auckland, New Zealand

ARTICLE INFO

Keywords:
Central America
Bayesian approach
Mean catchment elevation
Mean recharge elevation
Isotopic fractionation
Water resource

ABSTRACT

Study region: Central America
Study focus: Knowledge of the mean recharge elevation (MRE) of water resources is important where water resources are vulnerable. The purpose of this study was to develop and apply a Bayesian approach which incorporates isotopic uncertainties and evaporative effects on isotopic compositions to determine the MRE of 680 surface water sources from Central America. Differences were assessed between results from our approach and those from other isotope-based methods that do not account for these factors.
New hydrological insights for the region: Different MRE patterns were identified for Pacific and Caribbean basins, which were characterized by distinct isotopic signatures: 1) the Pacific slope had recharge occurring at higher elevations relative to the source mean catchment elevation (MCE) and 2) the Caribbean slope had recharge largely occurring at elevations lower than the MCE. These relationships were quantified: $MRE_P = 1.072\ (MCE) + 45.65$ (Pacific: $r^2 = 0.93$, error = 144 m); $MRE_C = 0.9493\ (MCE) - 28.24$ (Caribbean: $r^2 = 0.83$, error = 190 m). The MRE, surface water site elevation (SWSE), and MRE-SWSE differences were generally greater on the Pacific slope, which hosts most of the region's population. Bayesian MRE estimates were on average lower than MREs obtained using other methods and may better approximate the actual (recharge-weighed) MRE, suggesting that the inclusion of isotopic uncertainties, evaporative corrections, and recharge likelihoods all positively effect MRE estimations.

* Corresponding author at: Department of Earth and Atmospheric Sciences, University of Houston, Science and Research Building 1 Room 214, 3507 Cullen Blvd, Houston, TX, 77204-5008, United States.
E-mail addresses: lnarellano@uh.edu (L.N. Arellano), stephen.good@oregonstate.edu (S.P. Good), ricardo.sanchez.murillo@una.cr (R. Sánchez-Murillo), todd.jarvis@oregonstate.edu (W.T. Jarvis), david.noone@auckland.ac.nz (D.C. Noone), finkenbc@oregonstate.edu (C.E. Finkenbiner).

https://doi.org/10.1016/j.ejrh.2020.100739
Received 21 February 2020; Received in revised form 24 July 2020; Accepted 26 August 2020
Available online 28 September 2020

1. Introduction

Information regarding spatial distributions of recharge and the factors that control these distributions is essential for water managers in the face of expanding populations, rapid urbanization, and changes in land use and climate. These stressors affect the quantity and quality of water available and therefore can have long-lasting social, political, and environmental implications (Cosgrove and Loucks, 2015). Mountainous regions are particularly sensitive to hydrologic modifications (Alexander et al., 2007; Diaz et al., 2003; Dodds and Oakes, 2008), and are often overlooked in policy and management plans due to their complicated topography and hydrological uncertainties such as those associated with runoff and recharge processes and how these processes respond to disturbances (Ariza et al., 2013; Křeček and Haigh, 2019). However, these regions contain headwaters distinguished for their role in recharging surface water and groundwater resources (Křeček and Haigh, 2000). They supply freshwater to a large portion of the world's population through discharge transported to lower-lying areas (contributing 20–50 % of the total discharge in humid areas and 50–90% in arid regions (Viviroli and Weingartner, 2004)) and also support approximately one-quarter of the world's terrestrial biological diversity (Spehn et al., 2010). As such, the characterization of recharge patterns across mountainous regions can help inform conservation and protection practices to ensure adequate freshwater supply and ecosystem services maintenance.

Topographic relief produces distinct gradients in the isotopic signatures of precipitation resulting from the altitude effect, or the phenomenon of $\delta\ ^{18}O$ and $\delta\ ^{2}H$ becoming more depleted with increasing elevation (Dansgaard, 1964). Consequently, stable isotopic lapse rates have been leveraged to provide insight into the spatial and temporal dynamics of recharge elevation in many mountainous regions (Ambach et al., 1968; Bhat and Jeelani, 2015; Eastoe and Towne, 2018; Gat and Dansgaard, 1972; Gonfiantini et al., 2001; Jeelani et al., 2018; Jung et al., 2019; Koeniger et al., 2017, 2016; Longinelli and Selmo, 2003; Matiatos and Alexopoulos, 2011; O'Driscoll et al., 2005; Paternoster et al., 2008; Sánchez-Murillo et al., 2016; Sánchez-Murillo and Birkel, 2016; Sappa et al., 2018; SaravanaKumar et al., 2010; Saylor et al., 2009; Siegenthaler and Oeschger, 1980; Vespasiano et al., 2015; Winckel et al., 2002; Yamanaka et al., 2015; Yamanaka and Yamada, 2017; Zhu et al., 2018). The lapse rates are typically determined based on the $^{18}O/^{16}O$ ($\delta^{18}O$) and $^{2}H/^{1}H$ ($\delta^{2}H$) ratios of precipitation collected at different elevations in the study area. As ^{18}O and ^{2}H can vary widely between rainfall events (Clark and Fritz, 1997), this method requires sampling over a long period of time (at least four years; Putman et al., 2019) and therefore can be inhibited by financial or logistical constraints (Longinelli and Selmo, 2003). An alternative approach, described as the "small spring method" (Vespasiano et al., 2015), involves sampling shallow groundwater from springs instead. The seasonal changes exhibited by groundwaters are minor, so they can be used to constrain the lapse rate in a shorter timeframe (i.e., one year or less; Sánchez-Murillo and Birkel, 2016). However, this method is only valid where the groundwater is immature, the springs have small upstream catchments, and there are small differences between the spring and the recharge elevations. Further studies have conducted spatial analysis of stable isotopes using Geographic Information Systems (GIS). Isoscapes (i.e., isotope landscape mapping; Bowen, 2010) have been shown to provide fairly accurate predictions when derived from the interpolation of geographically distributed isotopic observations or developed by process-level models to predict the isotopic composition at a given location (Bowen and Good, 2015). Models that include parameters relating isotopic compositions to climatic and/or geographic variables often outperform "space-only" interpolations (e.g., nearest neighbor, inverse distance-weighting, etc.), with errors reduced by 10–15 % (Bowen and Revenaugh, 2003). Yamanaka and Yamada (2017) thus used multiple regression to construct hydrogen and oxygen precipitation isoscapes for Central Japan, where $\delta^{18}O$ and $\delta^{2}H$ were functions of latitude, longitude, and elevation. Then the models were used to estimate the mean recharge elevations (MREs) of tap water sources.

Unrestricted to mountainous settings, different combinations of stable water isotopes $\delta^{18}O$ and $\delta^{2}H$, other geochemical tracers including ^{3}H, ^{14}C, and the noble gases (He, Ne, Ar, Kr, and Xe), hydrochemical data, and physical data have frequently been used together to inform geostatistical techniques (Lentswe and Molwalefhe, 2020), machine learning algorithms (Pourghasemi et al., 2020), and simulation models (da Costa et al., 2019; Meredith et al., 2011; Mosase et al., 2019) to constrain the spatial distribution of actual or potential groundwater recharge within catchments. Similar datasets have been combined to characterize factors which influence stream network discharge by identifying sources and seasonal dynamics of surface runoff (Tetzlaff et al., 2007) and river recharge (Guo et al., 2017) and to assess catchment water balances (Karim and Veizer, 2002). These combined approaches are often preferable to a single dataset approach, because each tracer and physically-based method is associated with significant uncertainties (Hall et al., 2020). For example, the current methods using stable isotopes do not consider uncertainties in measured isotopic compositions, and as these methods have mainly been applied to study groundwater sources, secondary processes occurring after precipitation are assumed to be insignificant. However, evaporative fractionation can occur in the soil during infiltration and affect original isotopic compositions (Sánchez-Murillo and Birkel, 2016; Sprenger et al., 2017; Vespasiano et al., 2015; Winckel et al., 2002).

Our primary objective was to develop a probabilistic interpretation of the approach outlined in Yamanaka and Yamada (2017) that captures both the uncertainties in isotopic values as well as potential isotope fractionation due to evaporation. First, we developed a statistical method for estimating the MRE of groundwater and surface water sources by incorporating stable isotopic compositions within a Bayesian framework. In the surface water context, mean "recharge" elevation refers to instances where precipitation is directly contributing water to streams. Second, we applied our approach to estimate the MRE of surface water samples collected from streams in Panama, Costa Rica, Nicaragua, Honduras, and El Salvador and examined regional MRE patterns as well as relationships between MRE and catchment properties. Third, we compared resulting MREs to those obtained using simpler isotope-based methods. The differences between estimated MREs and sample elevations were also calculated as justification for improved management of mountainous regions. The results can inform governmental institutions and non-governmental organizations in Central America and raise awareness regarding conservation and protection of critical recharge zones. The methods developed here may also contribute to the understanding of recharge dynamics in other regions where isotopically informed geospatial models are becoming robust and more

widely applied to improve water resources planning (Dehaspe et al., 2018; Jasechko and Taylor, 2015; Taylor et al., 2012; Villegas et al., 2018).

2. Materials and methodology

2.1. Study area

The Central American countries of Panama, Costa Rica, Nicaragua, Honduras, and El Salvador are located between 7° and 16 °N latitude and 77° and 90 °W longitude (Fig. 1). These countries constitute 74.87 % of the total land area and ~65 % of the total population of Central America. Central America has a total land area just over 524,000 km^2 and is home to more than 47 million people. Over 27 million people currently live in urban areas (mainly in the Pacific domain), but at modern rates of population growth and urbanization, an additional 25 million are predicted to live in cities by 2050 (Maria et al., 2017). Although there have always been restrictions on certain high-risk activities in recharge areas, deliberations to regulate urban expansion in these areas are incipient. Many of the region's surface water resources are already degraded due to indiscriminate urban and industrial waste disposal, as well as uncontrolled agricultural-related activities such as deforestation (Castillo et al., 1997; Parello et al., 2008; Silva et al., 2015). As a result, the region is highly dependent on groundwater extraction (estimated at ~1.9×10^{10} $m^3 yr^{-1}$), however, virtually all of the aquifers supplying Central American metropolitan areas indicate overexploitation (Ballestero et al., 2007).

The region is also characterized by an unequal distribution of water both spatially and temporally. A volcanic arc that extends north to south across the region divides Central America into Pacific and Caribbean draining basins. The Caribbean slope drains 70 % of the region and has the largest rivers and watersheds, however ~70 % of the population lives on the Pacific slope, where there is higher economic activity (Leonard, 1987). On the Pacific slope, heavy rains and river flows occur mainly between May and November. The beginning of the rainy season in May is associated with the latitudinal migration of the Intertropical Convergence Zone (ITCZ) over the Central America region, which leads to the development of convective activity and cyclonic circulation. By July and August, the ITCZ has moved north of the region causing precipitation to decrease along the Pacific coast, known as the mid-summer drought or MSD. At the same time, precipitation increases to a maximum along the Caribbean slope resulting from orographic forcing of Caribbean-sourced moisture transported directly across the region by the northeast trade winds (Magaña et al., 1999). The Caribbean

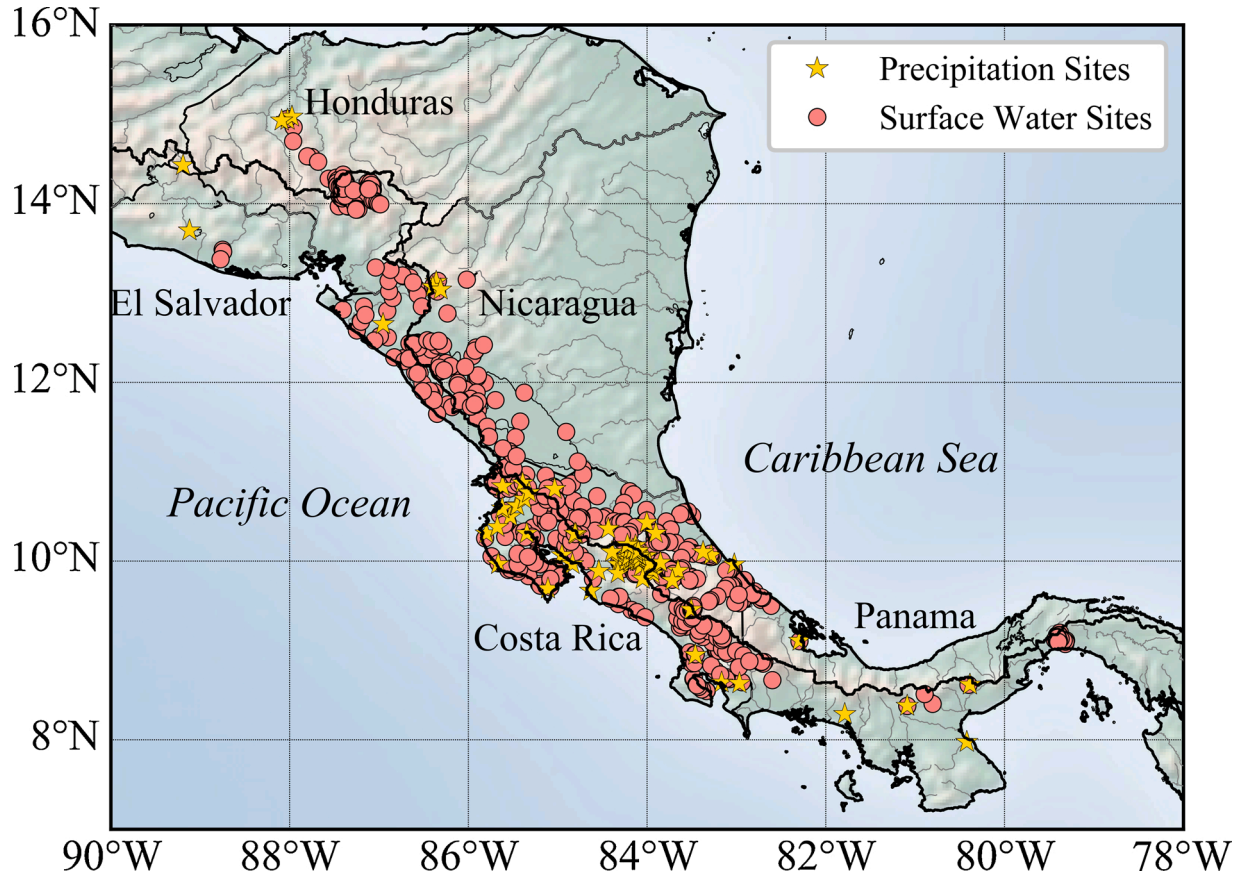

Fig. 1. Map of the study area indicating sampling sites, including precipitation sites (yellow stars) and surface water sites (pink circles). The black line extending parallel to the Pacific coastline represents the volcanic arch that divides the region into Pacific and Caribbean basins.

Sea provides the dominant source of moisture to the region (Durán-Quesada et al., 2010) so that the Caribbean slope experiences a relatively homogeneous precipitation regime throughout the year. It receives greater annual rainfall than the Pacific slope, which experiences a rain shadow effect due to the presence of the central mountain range. These contrasting precipitation modes reflect the interaction of sea-surface temperatures (SSTs), air circulation processes, and topography, which are the primary controls on regional climate (Sáenz and Durán-Quesada, 2015; Taylor and Alfaro, 2005). Temperature varies from the coastal lowlands to the mountains, but seasonal fluctuations in temperature are low (<3 °C). Regional climate projections suggest the following changes by 2050: 1) a rainfall decrease (10–25 %) during the wet season (i.e. May to November) (Imbach et al., 2018); 2) a spatial extension of the area affected by the MSD (Magaña et al., 1999; Maldonado et al., 2013; Maurer et al., 2017; and 3) positive trends in temperature and dry extreme events, resulting in a net decrease of water availability (Imbach et al., 2018).

2.2. Stable isotope datasets

Stable isotope archives comprised of averaged annual amount-weighted precipitation ratios from 73 sites and averaged surface water ratios from 677 sites across Costa Rica, Nicaragua, Honduras, El Salvador, and Panama were compiled from recent studies (Sánchez-Murillo et al., 2020, 2016, 2013; Sánchez-Murillo and Birkel, 2016). A detailed description of these archives was provided by Sánchez-Murillo et al. (2020).

New stable isotope data of precipitation (N = 54; monthly composite samples from 5 sites) and surface waters (N = 37; monthly samples from 3 sites) were collected in Panama from July 2017 to July 2018. Rainfall totalizers were crafted to collect and preserve rainfall within the monthly period (IAEA, 2014). Each totalizer consisted of a 6-cm radius funnel and a 1-L, high-density polyethylene (HDPE) collection bottle. Calculated *d*-excess values were in agreement with the archived data values, which range from +2.9 to +14.4‰. Collection bottles were emptied into 5-L HDPE accumulation bottles, which were stored at room temperature until the end of the month. Then, a portion of the cumulative rainfall was transferred to a 16-mL glass E-C borosilicate sample bottle (Wheaton Science Products, USA). Sample bottles were sealed with parafilm and labeled with the site's name and the amount of precipitation collected for that month, calculated as: ppt (mm) = 10 V/(πr_f^2) where V is water volume collected (mL) and r_f is funnel radius (cm). The annual amount weighted ratio (δ_{P-AW}) for each new precipitation site was calculated as:

$$\delta_{P-AW} = \frac{\sum_{i=1}^{n} P_i \delta X_{P(i)}}{\sum_{i=1}^{n} P_i} \quad (1)$$

where n is the number of months, P_i is the monthly precipitation and $\delta X_{P(i)}$ is the δ^2H or $\delta^{18}O$ composition of precipitation for the *i*-th month. Surface water samples were collected from streams only at flowing sections to circumvent evaporative signals and base flow conditions were targeted to ensure that the sample was representative of cumulative upstream outflow (Sánchez-Murillo and Birkel, 2016). The annual amount weighted precipitation isotope ratio for each surface water site was calculated. Fig. 1 indicates the locations

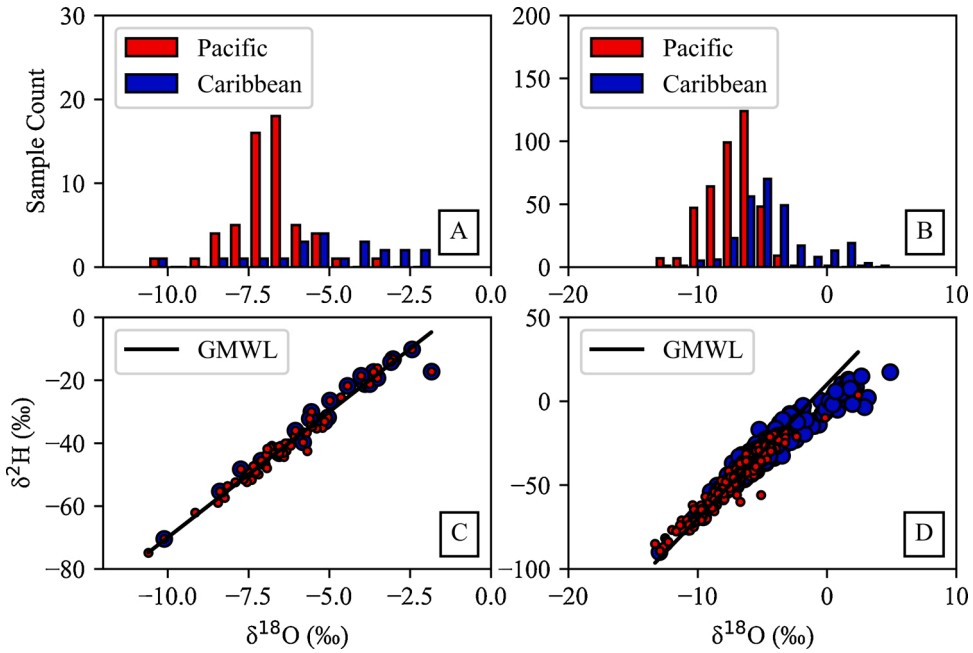

Fig. 2. The distribution of $\delta^{18}O$ (‰) in precipitation (a) and surface waters (b) by slope and the linear relationship between $\delta^{18}O$ and δ^2H in precipitation (c) and surface waters (d) for both slopes; the black line represents the global meteoric water line (GMWL), and Pacific and Caribbean samples are denoted by red and blue color, respectively.

of precipitation and surface water sites within the study area. There were 56 precipitation and 408 surface water sampling sites in the Pacific domain and 22 precipitation and 272 surface water sampling sites in the Caribbean domain. Isotopic signatures at each site were tested against the standard normal distribution. Fig. 2 illustrates the distributions of $\delta^{18}O$ in precipitation (a) and surface waters (b), as well as the relationships between $\delta^{18}O$ and $\delta^{2}H$ in precipitation (c) and surface waters (d) for both slopes (i.e., Pacific and Caribbean).

The new samples from Panama were analyzed at Oregon State University using a Cavity Ring Down Spectroscopy (CRDS) isotope analyzer L2120-*i* (Picarro, USA). All isotopic compositions were expressed in δ notation: $\delta = (R/R_{std} - 1)$, where R is the ratio of rare to abundant isotopes in the sample and R_{std} is the ratio of rare to abundant isotopes in Vienna Standard Mean Ocean Water (VSMOW). All δ values were reported in per mil (parts per thousand, ‰). Laboratory standards established using mass spectrometer measurements of Florida ($\delta^{2}H = -3.56‰$, $\delta^{18}O = -0.95‰$) and Boulder ($\delta^{2}H = -120.68‰$, $\delta^{18}O = -16.00‰$) tap waters were used to normalize the results to the VSMOW-VSLAP scale. Each sample was injected six times to compensate for memory effects, and the final three injections were averaged after correction to provide the measurement. The average analytical precision was ± 0.20‰ (1σ) for $\delta^{2}H$ and ± 0.05‰ (1σ) for $\delta^{18}O$.

2.3. Precipitation isotope ratio model

Multivariate regression models were constructed for $\delta^{2}H$ and $\delta^{18}O$ using the annual amount weighted precipitation isotope ratios. Following Yamanaka and Yamada (2017), the models included longitude (x), latitude (y), and elevation (z) of precipitation sites as potential explanatory variables for δ. Polynomial forms of the longitude, latitude, and elevation terms (x, x^2, x^3, y, y^2, y^3, z, z^2, z^3) were evaluated because the relationship between these variables and δ is not always linear (Yamanaka et al., 2015). Interaction terms (xy, xz, yz) were also assessed to gain an understanding of variable inter-relationships and their effect on δ.

2.4. Catchment extraction

Catchments for each surface water sample were obtained using 30 arc-second (grid cells of approximately 1 km^2) HydroSHEDS data (Lehner et al., 2008) within Pysheds (0.2.6), a Python package designed for watershed delimitation, stream network extraction, and determination of flow direction and accumulation. The longitude and latitude of each surface water site was employed as an outlet point to delineate the total upstream area contributing water flow to that point. The coordinates were directed to snap to the nearest cell having more than 20 upstream places. This criterion was included to adjust for any inaccuracies associated with input data (i.e., sample longitude, latitude, and elevation) that could result in an outlet point input not intersecting an actual water source. Once a catchment was delineated, all of the locations (L_j composed of x_j, y_j, and z_j) within it were extracted, and catchment properties, including a mean catchment longitude (x_j), latitude (y_j), and elevation (z_j) were calculated. Then, for each catchment location $L_j(x_j, y_j, z_j)$, an annual amount weighted precipitation isotopic composition $\widehat{\delta}_{P-AW(j)}$ was predicted using the precipitation model.

2.5. Assumptions in the mean recharge elevation assessment

2.5.1. Steady-state evaporation

The likelihood that the measured isotopic composition of a surface water sample was consistent with the isotopic composition of precipitation predicted at each location in its catchment was assessed within a Bayesian framework (Good et al., 2014). Following Yamanaka and Yamada (2017), it was assumed that the isotopic composition of surface water samples taken from different sources reflects approximately that of precipitation at their recharge areas plus Δ, which represents the isotope fractionation that occurs as a result of phase changes: $\delta_S = \delta_P + \Delta$. When there is a phase change, the heavy and light isotopes are partitioned relatively between the two phases. During evaporation, the light H and O isotopes are lost from the liquid water body preferentially and the remaining water becomes enriched in the heavier isotopes. This evaporative enrichment occurs along a slope which deviates from that of the global meteoric water line (Gibson et al., 2008). The evaporation line, $g()$, was defined as a function providing the $\delta^{2}H$ value for a given $\delta^{18}O$ value of t:

$$g\left(t\middle|X_{p(j)},\ Y_{p(j)},\ X_{*(j)},\ Y_{*(j)}\right) = \left(Y_{*(j)} - Y_{p(j)}\middle|X_{*(j)} - X_{p(j)}\right)\left(t - X_{p(j)}\right) + Y_{p(j)} \tag{2}$$

where the first parenthesized term on the right-hand side of the equation is the slope, $X_{p(j)}$ and $Y_{p(j)}$ are the $\delta^{18}O$ and $\delta^{2}H$ values of predicted precipitation at location j, and $X_{*(j)}$ and $Y_{*(j)}$ are the limiting $\delta^{18}O$ and $\delta^{2}H$ values of an evaporating water body under local climatological conditions (e.g., the final isotopic composition of the water sample as its volume approaches zero) at location j. The limiting isotopic composition was calculated as:

$$\delta_* = \frac{h\delta_A + \varepsilon}{h - \varepsilon \cdot 10^{-3}} \tag{3}$$

where ε is the total isotopic separation factor that includes both equilibrium and kinetic components, h is often assumed to be the relative humidity, and δ_A is the atmospheric composition of vapor (Gibson et al., 2016; Gibson and Edwards, 2002). Values for δ_A were estimated assuming isotopic equilibrium between atmospheric vapor and precipitation, since global-scale isotopic measurements of water vapor at ground level have revealed for most cases vapor-precipitation equilibrium is maintained over continental masses (Araguás-Araguás et al., 2000):

$$\delta_A = \frac{\delta_P - \varepsilon^+}{\left(1 + 10^{-3} \cdot \varepsilon^+\right)} \approx \frac{(1000 + \delta_P)}{\alpha^+} - 1000 \tag{4}$$

where ε^+ is the equilibrium isotopic separation, α^+ is the equilibrium fractionation, and ε^+ is related to α^+ by $\varepsilon^+ = (\alpha^+ - 1) \cdot 1000$ (Gibson et al., 2016; Gibson and Edwards, 2002). If the vapor and precipitation are in equilibrium, their isotopic-exchange reaction rates are well-known for a given temperature. The ε, h, and δ_A parameters used to determine limiting isotopic compositions were calculated using gridded WorldClim 2 data of average and minimum temperature at a 30 arc-second resolution (Fick and Hijmans, 2017). Given the humid conditions of the region, minimum temperature could be used as a proxy for dew point in h calculations (Gunawardhana et al., 2017).

2.5.2. Precipitation

Precipitation and its limiting composition at each location ($L_{(j)}$) in the catchment from which a surface water sample was collected was assumed to be from a normal distribution $\mathbf{d_{pj}} = [\mathbf{m_{pj}}, \mathbf{s_p}]$ with a mean ($\mathbf{m_{pj}}$) and covariance matrix ($\mathbf{s_p}$):

$$\mathbf{m_{pj}} = \left[\, \mu\left(\delta^{18}\mathrm{O}\right)_{p(j)} \quad \mu\left(\delta^{2}\mathrm{H}\right)_{p(j)} \quad \mu\left(\delta^{18}\mathrm{O}\right)_{*(j)} \quad \mu\left(\delta^{2}\mathrm{H}\right)_{*(j)} \,\right] \tag{5a}$$

$$\mathbf{s_p} = \begin{bmatrix} \sigma^2\left(\delta^{18}\mathrm{O}\right)_p & \sigma\left(\delta^{18}\mathrm{O},\ \delta^{2}\mathrm{H}\right)_p & 0 & 0 \\ \sigma\left(\delta^{18}\mathrm{O}, \delta^{2}\mathrm{H}\right)_p & \sigma^2\left(\delta^{2}\mathrm{H}\right)_p & 0 & 0 \\ 0 & 0 & \sigma^2\left(\delta^{18}\mathrm{O}\right)_* & \sigma\left(\delta^{18}\mathrm{O},\ \delta^{2}\mathrm{H}\right)_* \\ 0 & 0 & \sigma\left(\delta^{18}\mathrm{O},\ \delta^{2}\mathrm{H}\right)_* & \sigma^2\left(\delta^{2}\mathrm{H}\right)_* \end{bmatrix} \tag{5b}$$

where $\mu(\delta^{18}\mathrm{O})_{p(j)}$ and $\mu(\delta^{2}\mathrm{H})_{p(j)}$ are the $\delta^{18}\mathrm{O}$ and $\delta^{2}\mathrm{H}$ values predicted by the precipitation model at that location in the catchment and $\sigma^2(\delta^{18}\mathrm{O})_p$, $\sigma^2(\delta^{2}\mathrm{H})_p$, and $\sigma(\delta^{18}\mathrm{O}, \delta^{2}\mathrm{H})_p$ were fixed according to the model uncertainty (0.75, 52.18, and 5.97, respectively). The terms $\mu(\delta^{18}\mathrm{O})_{*(j)}$ and $\mu(\delta^{2}\mathrm{H})_{*(j)}$ are the $\delta^{18}\mathrm{O}$ and $\delta^{2}\mathrm{H}$ values of the limiting composition with associated uncertainties $\sigma^2(\delta^{18}\mathrm{O})_*$, $\sigma^2(\delta^{2}\mathrm{H})_*$, and $\sigma(\delta^{18}\mathrm{O}, \delta^{2}\mathrm{H})_*$. Since it was assumed that the atmospheric vapor is in equilibrium with local precipitation, the same variance and covariance values associated with the precipitation model were utilized.

2.5.3. Surface waters

Similarly, each surface water sample was assumed to be from a normal distribution $\mathbf{d_s} = [\mathbf{m_s}, \mathbf{s_s}]$ with a mean ($\mathbf{m_s}$) and covariance matrix ($\mathbf{s_s}$):

$$\mathbf{m_s} = \left[\, \mu\left(\delta^{18}\mathrm{O}\right)_s \quad \mu\left(\delta^{2}\mathrm{H}\right)_s \,\right] \tag{6a}$$

$$\mathbf{s_s} = \begin{bmatrix} \sigma^2\left(\delta^{18}\mathrm{O}\right)_s & 0 \\ 0 & \sigma^2\left(\delta^{2}\mathrm{H}\right)_s \end{bmatrix} \tag{6b}$$

where $\mu(\delta^{18}\mathrm{O})_s$ is the measured $\delta^{18}\mathrm{O}$ value of the surface water sample with analytical uncertainty $\sigma^2(\delta^{18}\mathrm{O})_s$ and $\mu(\delta^{2}\mathrm{H})_s$ is the measured $\delta^{2}\mathrm{H}$ value of the surface water sample with analytical uncertainty $\sigma^2(\delta^{2}\mathrm{H})_s$. Uncertainties were fixed at 0.05‰ and 0.20‰ respectively, based on the uncertainty of the CRDS analysis.

2.6. Bayesian likelihood assessment

In statistics and probability theory, Bayes law is used to determine the conditional probability of events based on prior knowledge of the conditions that might be relevant to the event. As it shows the relationship between a conditional probability and its reverse form, it can be used to invert a conditional probability. In this study, the likelihood that a surface water sample recharged at a particular location within its catchment was assessed through an approach modified from Good et al. (2014) and Kennedy et al. (2011):

$$P(L_j|\delta_s) = \frac{\mathrm{P}\left(\delta_s|\mathrm{L}_j\right)\mathrm{P}(\mathrm{L}_j)}{\int \mathrm{P}\left(\delta_s|\mathrm{L}_j\right)\mathrm{P}(\mathrm{L}_j)} \tag{7}$$

where the posterior distribution, $P(L_j|\delta_s)$, expresses the probability that a particular catchment location $L_{(j)}$ with a normal predicted precipitation distribution $\mathbf{d_{pj}}$ served as the location of recharge for a collected surface water sample δ_s with a normal sample distribution $\mathbf{d_s}$. The prior probability distribution $P(L_j)$ defines the probability of that location within the catchment; in this case, prior knowledge assumed that every location has equal likelihood of occurrence. The conditional probability, $\mathrm{P}\left(\delta_s|\mathrm{L}_j\right)$, is the probability of obtaining the surface water sample δ_s with a normal sample distribution $\mathbf{d_s}$ given the location $L_{(j)}$ with a normal predicted precipitation distribution $\mathbf{d_{pj}}$. The conditional probability was determined by integrating the sample distribution, $f\mathbf{d_s}$, along potential evaporation lines *(g(t))* and multiplying these integrated values by the probability that a particular evaporation line occurs, $f\mathbf{d_{pj}}$:

$$P\left(\delta_s L_j\right) = \int\int\int\int f\mathbf{d_{pj}}\left(X_{p(j)},\ Y_{p(j)},\ X_{*(j)},\ Y_{*(j)}\right) \int_{X_{pj}}^{X_{*j}} g'(t) f\mathbf{d_s}(t,\ g(t))\, dt\, dx_{p(j)} dy_{p(j)} dx_{*(j)} dy_{*(j)} \tag{8}$$

This approach integrates t from $X_{p(j)}$ to $X_{*(j)}$, examining all possible evaporative enrichments along evaporation lines with all

possible predicted precipitation and limiting isotopic composition endpoints ($X_{p(j)}$, $Y_{p(j)}$ and $X_{*(j)}$, $Y_{*(j)}$) and their probability of occurring ($f\mathbf{d_{pj}}$) against the probability of a given value of the sample occurring ($f\mathbf{d_s}$). If $f\mathbf{d_{pj}}(\mathbf{x})$ is a normal distribution with a mean ($\mathbf{m_{pj}}$) according to isotope values predicted by the model at that location and a covariance matrix ($\mathbf{s_p}$) according to model uncertainty, it is given by:

$$f\mathbf{d}_{\mathrm{pj}}(\mathbf{x}) = \frac{1}{\sqrt{2\pi^k|\mathbf{s_p}|}}\exp\left(-\frac{1}{2}(\mathbf{x}-\mathbf{m}_{\mathrm{pj}})^T\mathbf{s_p}^{-1}(\mathbf{x}-\mathbf{m}_{\mathrm{pj}})\right) \tag{9}$$

$P(\delta_s||L_j)$ was then evaluated over n = 500 realizations as:

$$P(\delta_s|L_j) = \sum_{l=1}^{n}\frac{1}{n}\sum_{t=x_l}^{x*_j}\frac{\Delta t\sqrt{1+\left(\frac{l_{y*(j)}-l_{yp(j)}}{l_{x*(j)}-l_{xp(j)}}\right)^2}}{2\pi\sigma_{(\delta^{18}\mathrm{O})s}\sigma_{(\delta^2\mathrm{H})s}}\exp\left(-\frac{(t-\mu_{(\delta^{18}\mathrm{O})s})^2}{2\,\sigma^2_{(\delta^{18}\mathrm{O})s}}\frac{\left(\left(\frac{l_{y*(j)}-l_{yp(j)}}{l_{x*(j)}-l_{xp(j)}}\right)(t-x_l)+y_l-\mu_{(\delta^2\mathrm{H})s}\right)^2}{2\,\sigma^2_{(\delta^2\mathrm{H})s}}\right) \tag{10}$$

where $l_{xp(j)}$, $l_{yp(j)}$, $l_{x*(j)}$, and $l_{y*(j)}$ are the lth realizations of predicted precipitation and limiting water drawn from $\mathbf{d_{pj}}$. Here Δt was specified as to ensure that the Riemann sum adequately approximated the inner integral in Eq. 8. This approach was executed using a Python script included in the supplementary material. For an illustration of this approach, see Fig. 4 of Good et al. (2014). Assuming that the prior probability distribution $P(L_j)$ is uniform, the form of Bayes Law was simplified as:

$$P(L_j|\delta_s) = \frac{P(\delta_s|L_j)}{\sum_{x=1}^{j}P(\delta_s|L_j)} \tag{11}$$

and the relative likelihood that a particular location within the surface water sample catchment $L_{(j)}$ served as the location of recharge for a given sample δ_s was determined by normalizing the conditional probability. Fig. 3 demonstrates likelihood throughout a single catchment, using the Sixaola River Basin in southern Costa Rica as an example.

2.7. Calculation of mean recharge elevations

The MRE of the surface water sample was then calculated by weighting each catchment elevation by its respective probability and summing these products:

$$\mathrm{MRE} = \sum P(L_j|\delta_s)^* z_j \tag{12}$$

Similarly, the standard deviation of the recharge elevation (SDRE) is calculated as:

$$\mathrm{SDRE} = \sqrt{\left(\sum P(L_j|\delta_s)^* z_j^2\right) - \left(\sum P(L_j|\delta_s)^* z_j\right)^2} \tag{13}$$

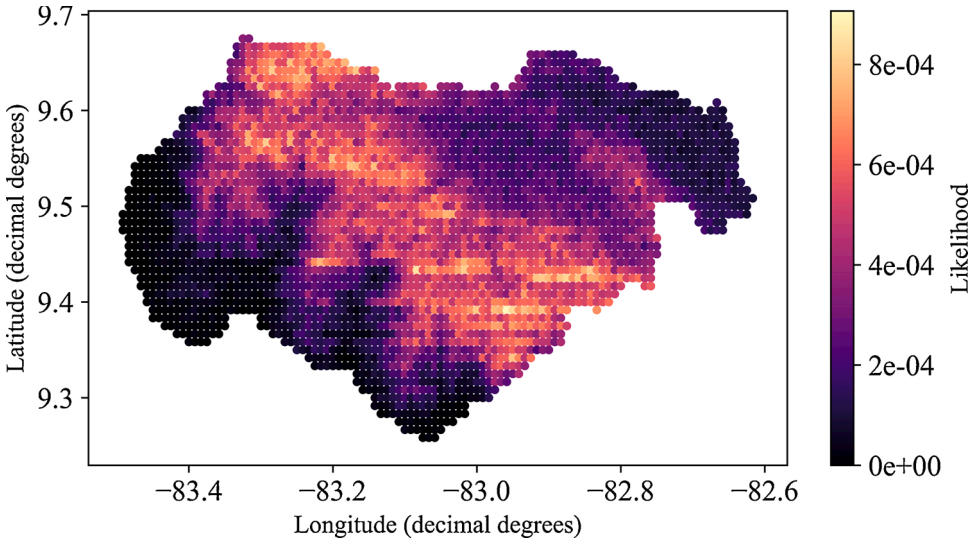

Fig. 3. Relative likelihood values for each location in the upstream catchment of a sample collected from the Sixaola River, Costa Rica. The sample has an estimated mean recharge elevation of ~818 m asl.

and the difference between the MRE and the surface water site elevation (SWSE or z_{min}, the contributing catchment's minimum elevation) was also calculated (i.e $z_{MRE-SWSE}$ = MRE - z_{min}).

3. Results

3.1. Precipitation isotope ratio model

Based on adjusted R^2 criterion, models were derived for δ^2H and $\delta^{18}O$ in precipitation where x is longitude (decimal degrees west), y is latitude (decimal degrees north), and z is elevation (meters above sea level, m asl):

$$\widehat{\delta}_{P-AW} = C_0 z 10^{-3} + C_1 y^3 + C_2 y^2 + C_3 y + C_4 x^2 + C_5 x + C_6 xy + C_7 \quad (14)$$

The z term represents the altitude and C_0 the local isotopic lapse rate. Since precipitation-producing air masses are mainly carried from the Caribbean Sea in a south-west direction by the trade winds, both the x and y terms can represent the continental effect, where $\delta^{18}O$ and δ^2H decrease inland from the coast. No latitude effect has been reported in the humid tropics, however, in Panama a "pseudo" latitude effect results from the collinearity of latitude with distance from the Caribbean Sea (Lachniet and Patterson, 2006). Fit model term coefficients are shown in Table 1. These models can estimate the isotopic composition of regional precipitation with mean absolute errors of 6.60‰ for δ^2H ($R^2_{adjusted} = 0.54$) and 0.80‰ for $\delta^{18}O$ ($R^2_{adjusted} = 0.57$). The most significant errors (> 2.0‰ for $\delta^{18}O$) are associated with sites located in NW Costa Rica along the Pacific slope of the mountainous divide (Fig. 4), a region characterized by relatively small precipitation events and large secondary evaporation processes. In order to further examine the performance of our precipitation model, the Online Isotopes in Precipitation Calculator (OIPC) (Bowen, 2017; Bowen and Revenaugh, 2003) was also used to determine mean annual $\delta^{18}O$ and δ^2H values for the locations associated with precipitation samples and model errors were compared. The OIPC estimates $\delta^{18}O$ and δ^2H based on the interpolation of global data derived primarily from the Global Network for Isotopes in Precipitation (GNIP) database (IAEA/WMO, 2015), and the interpolation is based on a composite model that includes latitude and altitude parameters to represent temperature effects as well as a distance-weighting parameter to account for variability in $\delta^{18}O$ and δ^2H not resolved by the other parameters (Bowen and Revenaugh, 2003). The OPIC predicted regional precipitation compositions with mean absolute errors of 11.11‰ for δ^2H and 1.37‰ for $\delta^{18}O$.

3.2. Mean recharge elevations

The model-predicted $\delta^{18}O$ and δ^2H values for the locations in a sample's catchment were used to evaluate the probabilities that each location served as a location of recharge, enabling the calculation of the sample's MRE (Fig. 5). The MRE for 46.5 % (316) of the surface water samples was higher than 1000 m asl. Of the 316 samples recharged above 1000 m asl, 235 (74.4 %) were derived from a Pacific catchment. Additionally, the MRE for 13.1 % (89) of the surface water samples was higher than 2000 m asl, with 72 of the 89 (80.9 %) having been derived from a Pacific catchment. Those surface water sources recharged above 2000 m asl were all located in the mountainous interior of northeast Panama and Costa Rica and along the Pacific coast of Costa Rica. The elevational distribution of MRE for surface water sources by slope is shown in Fig. 6. While the MRE of Pacific samples was widely distributed across different elevations, 50.4 % (137) of the Caribbean samples (representing 20.1 % of all 680 samples) recharged at an elevation below 500 m asl. The distributions of MRE, SWSE, and the differences between MRE and SWSE ($z_{MRE-SWSE}$) by slope are compared in Fig. 7. MREs and SWSEs were higher on the Pacific slope, and the average difference between MREs and SWSEs on the Pacific slope (531.2 m) was 78.7 m higher than on the Caribbean slope (452.5 m).

4. Discussion

4.1. Assessment of MRE uncertainties

One advantage of the Bayesian approach implemented in this study was the ability to assess the uncertainties associated with the MRE estimates. The standard deviations of the recharge elevations (SDREs) range from 0 to ~823 m with a mean value of 241 m. The lowest SDREs (generally ≤241 m) were associated with the MRE estimates of samples from El Salvador (σ_{mean} = 158 m), Honduras

Table 1
Precipitation model parameters.

Parameter (Unit)	δ^2H	$\delta^{18}O$
C_0 (‰ km^{-1})	−1.09E+1	−1.48E0
C_1 (‰ DD^{-3})	6.48E-1	6.33E-2
C_2 (‰ DD^{-2})	−2.73E+1	−2.81E0
C_3 (‰ DD^{-1})	−1.92E+2	−2.45E+1
C_4 (‰ DD^{-2})	−2.73E0	−3.03E-1
C_5 (‰ DD^{-1})	−3.81E+2	−4.18E+1
C_6 (‰ DD^{-1})	−6.68E0	−7.61E-1
C_7 (‰)	−1.44E+4	−1.56E+3

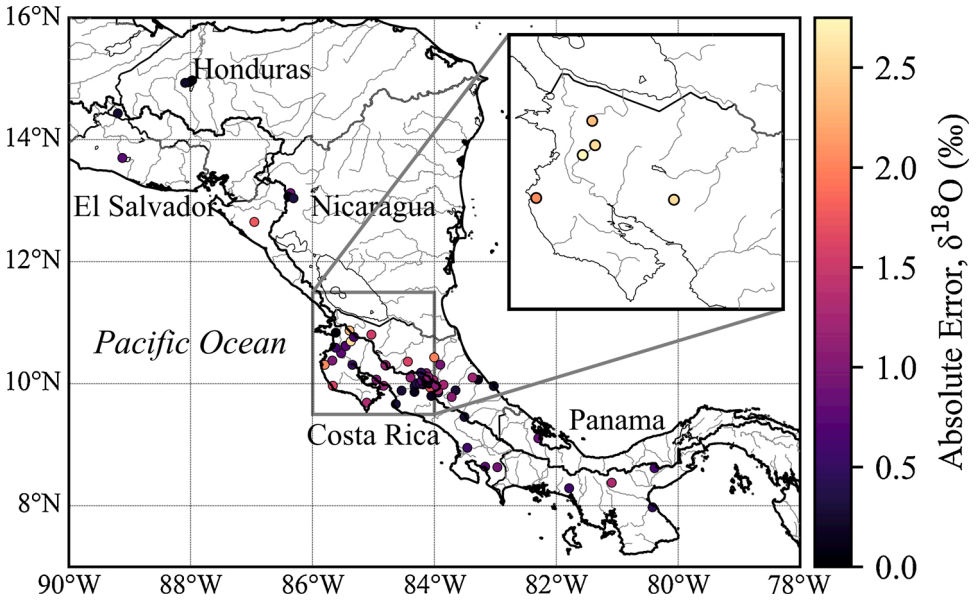

Fig. 4. Map showing the absolute error of modeled $\delta^{18}O$ (‰) for each precipitation site. The map inset shows those sites with absolute errors greater than 2.0 permil.

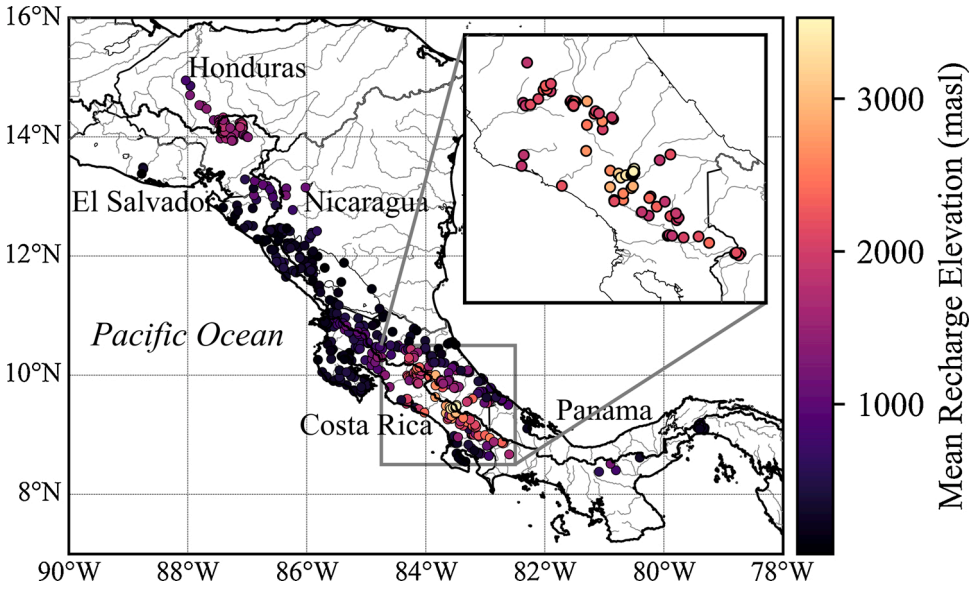

Fig. 5. Map showing the estimated mean recharge elevation of each surface water sample. The map inset shows those sites with mean recharge elevations above 2000 m asl.

(σ_{mean} = 187 m), Nicaragua (σ_{mean} = 178 m), and Panama (σ_{mean} = 198 m). Meanwhile, the MRE estimates of samples from both Pacific and Caribbean domains of Costa Rica are associated with higher SDREs (σ_{mean} = 286 m) (Fig. 8). Significant trends ($p < 0.0001$) of SDRE with mean catchment elevation and catchment relief (defined as z_{max} - z_{min}) were found for both slopes across the region, suggesting that the complex topography may help explain the observed spatial variability in SDRE. It is possible our precipitation model's assumption of a spatially uniform isotopic lapse rate could be a cause of greater SDRE. Altitude effects have been found to differ for Pacific versus Caribbean domains in countries within and near the study area, with isotopic lapse rates varying between -0.50 to -1.9‰ km^{-1} on the Pacific slope while increasing up to -2.4‰ km^{-1} on the Caribbean slope (Lachniet et al., 2007; Lachniet and Patterson, 2009; Perez et al., 2015; Sánchez-Murillo et al., 2020; Wassenaar et al., 2009). As SDRE was found to correlate strongly with sampling elevation only on the Caribbean slope and with catchment size only on the Pacific slope, the mechanisms responsible for spatial variations in MRE uncertainty may ultimately vary depending on domain and warrant further investigation.

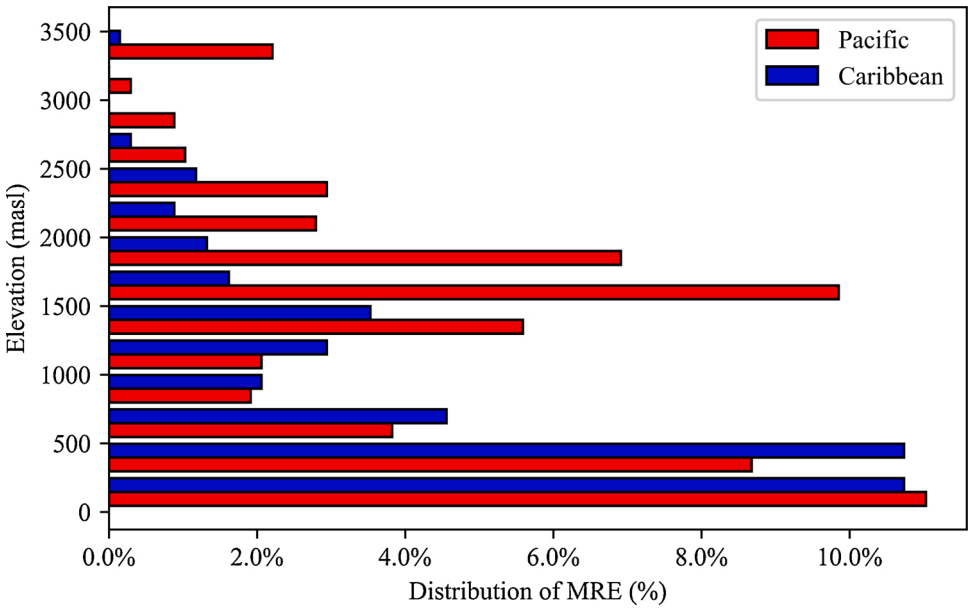

Fig. 6. The elevational distributions of mean recharge elevations by slope.

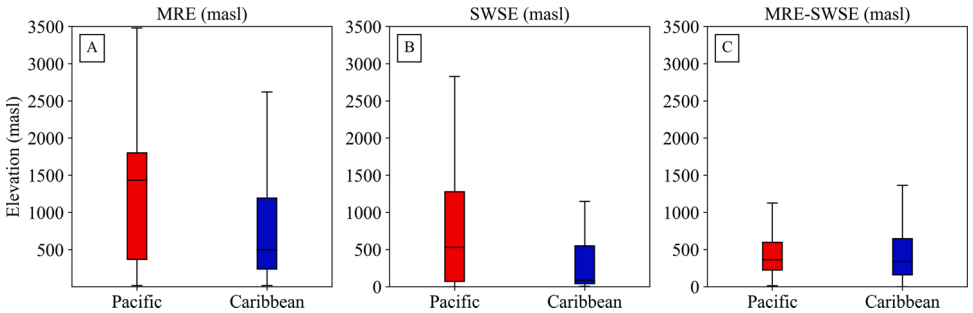

Fig. 7. A comparison of the elevational distributions of mean recharge elevations (MRE), surface water site elevations (SWSE), and MRE-SWSE differences between slopes.

4.2. Cross-validation of MRE estimates

In order to examine how MREs have changed with the incorporation of Bayesian probabilities, the MREs of surface water samples were also estimated using the isoscape approach presented in Yamanaka and Yamada (2017), hereafter YY17. The YY17 approach estimates MREs using a regional isotopic lapse rate, Γ (‰ · km^{-1}, corresponding to the C_0 model parameter in Eq. 14), and isotopic shift, Δ (‰):

$$\mathrm{MRE}_{\mathrm{YY17}} = \frac{10^3\left(\delta_{SW} - \delta_P^* - \Delta\right)}{\Gamma} \tag{15}$$

where δ_{SW} is the measured $\delta^{18}O$ or δ^2H of the surface water sample and δ_P^* is the sea level $\delta^{18}O$ or δ^2H value of precipitation at given coordinates. The δ_P^* parameter is derived from the precipitation model:

$$\delta_P^* = \widehat{\delta}_{P-AW} - \Gamma z\, 10^{-3} = C_1y^3 + C_2y^2 + C_3y + C_4x^2 + C_5x + C_6xy + C_7 \tag{16}$$

and the Δ parameter is optimized via iteration so as to minimize the differences between annual precipitation-weighted mean catchment elevations ($\mathrm{MCE_{PW}}$) and estimated MREs, although the optimized case only improved the differences by 15–50 m relative to the case assuming Δ = 0 in the YY17 study. $\mathrm{MCE_{PW}}$ is used as a proxy for recharge-weighted MRE where recharge flux (precipitation minus evapotranspiration) cannot be determined due to uncertainties associated with estimating evapotranspiration.

Bayesian MRE values are on average 503 ($\delta^{18}O$-based) and 391 (δ^2H-based) m lower than MREs resulting from the YY17 approach assuming no isotopic shift occurred and 539 ($\delta^{18}O$-based) and 425 (δ^2H-based) m lower than the YY17 approach with optimized Δ

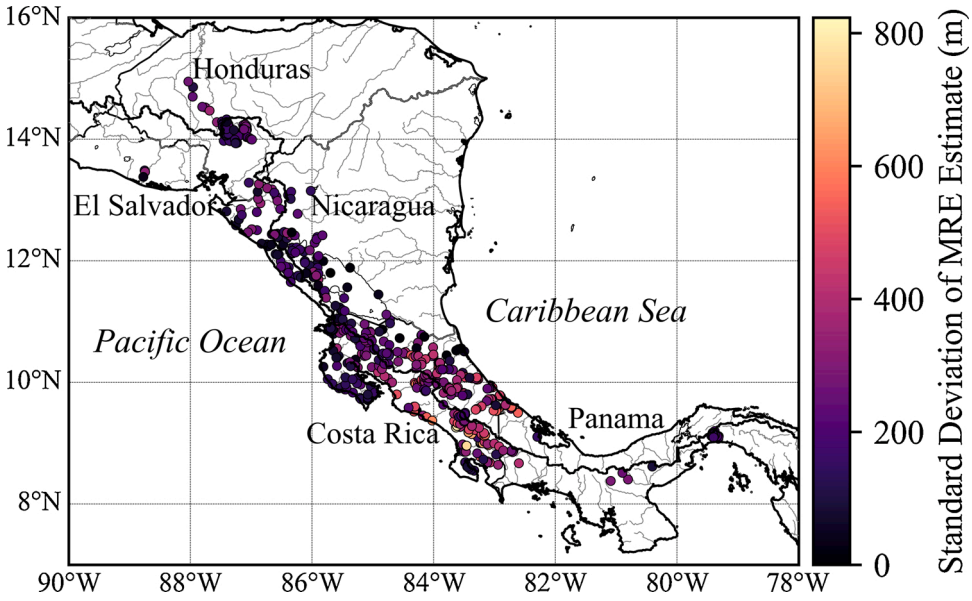

Fig. 8. Map showing the spatial variability of uncertainties in MRE estimates.

values. The incorporation of regional Δ values for $\delta^{18}O$ and $\delta^{2}H$ in the YY17 approach only affected the differences between samples' MRE estimates and MCE_{PW} by 6−67 m. However, the differences between YY17-derived MREs and MCE_{PW}s were generally much larger than those between Bayesian-derived MREs and MCE_{PW}s (Fig. 9). The Bayesian approach produces estimates of MRE that are on average 69 m higher than sample MCE_{PW}'s. Together, these trends illustrate how regional isotope data will yield MREs that are higher than samples' MCE_{PW}. They further demonstrate how an isotopic lapse rate-based method that does not also consider probabilities across a sample's catchment in the process of MRE determination will result in estimates less proximate to the sample's MCE_{PW}.

Bayesian MRE estimates for surface water samples from the Pacific slope of Costa Rica, Nicaragua, Honduras, and El Salvador were also compared on a broad-scale to those from Sanchez-Murillo et al. (2020), where MREs for Pacific ground water samples were calculated using a simple isotopic lapse rate method with no account for the potential effects of evaporative enrichment on isotopic

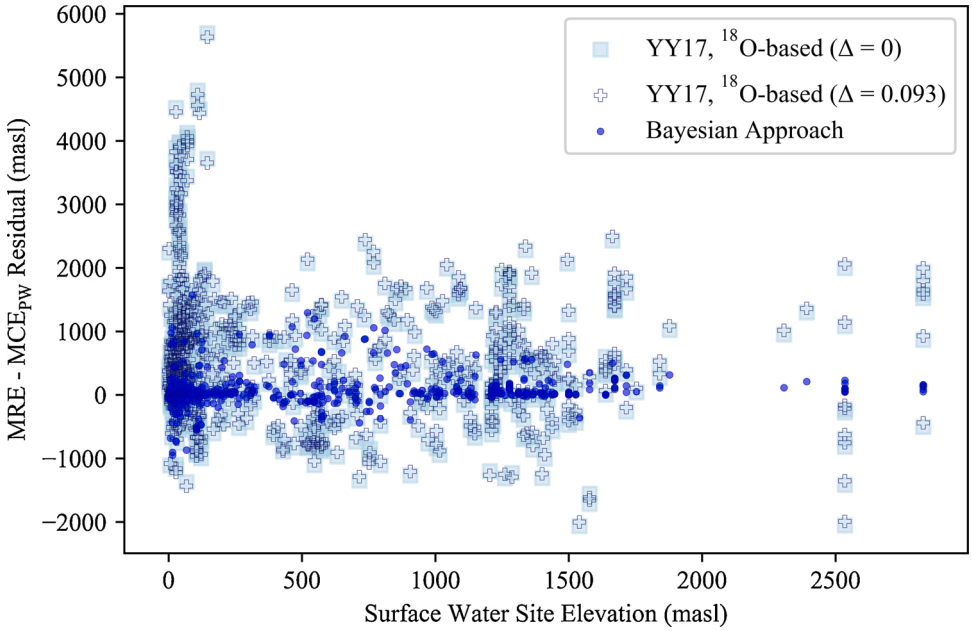

Fig. 9. A comparison of mean recharge elevation (MRE) - precipitation weighted mean catchment elevation (MCE_{PW}) residuals resulting from the Bayesian approach and two variations of the Yamanaka and Yamada (2017) approach, one where isotopic shift due to evaporative enrichment of samples is assumed to be zero and one where a regional ^{18}O-based value for isotopic shift was used.

compositions of the water samples. Since surface water samples for this study were collected from streams during base flow conditions, the patterns observed here can be representative of regional groundwater recharge as well (Sánchez-Murillo and Birkel, 2016). Median MREs for the Pacific domain of each country using the Bayesian and lapse rate-based approaches are compared in Table 2. With the exception of Honduras, countries' median MREs are again much lower according to the Bayesian approach, supporting the notion that the Bayesian statistical analysis will result in lower MRE estimates relative to the other isotope-based approaches assessed here. The $\delta^{18}O$ isotopic lapse rate of -1.48‰ km^{-1} derived from the precipitation model and used here in the probabilistic assessment of MREs was similar to the regional isotopic lapse rate of 1.0‰ km^{-1} which was used to estimate MREs in Sánchez-Murillo et al. (2020). It should be noted since the lapse rate from Sánchez-Murillo et al. (2020) was partially constructed using isotope data from historical rainfall stations, it is possible some of the ratios were affected by improper collection. Therefore, the lapse rate of 1.0‰ km^{-1} is likely lower than it would be based solely on more recent and robust monitoring sites, and it can be inferred that the additional constraints provided by the incorporation of isotopic uncertainties and evaporative effects are significant.

4.3. MRE and catchment properties

In this study, patterns of MRE were interpreted by assessing the relationship between MRE and catchment properties, including mean catchment longitude, mean catchment latitude, mean catchment elevation, minimum catchment elevation (SWSE), catchment relief, and catchment size. Changes in MRE with mean catchment longitude and latitude appear to reflect changes in SWSE (i.e., larger (smaller) MREs are associated with sampling locations of higher (lower) elevations; $p < 0.001$ for both slopes). A comparison of MRE and mean catchment elevation (MCE) demonstrates that samples collected from the Pacific slope generally have a MRE close to or above the MCE, while samples collected from the Caribbean slope tend to have a MRE near or below the MCE (Fig. 10). It is likely that these different relationships between MRE and MCE for the Pacific and Caribbean slopes are related to the distinct precipitation regimes characterizing them.

Previous studies have identified two main sources of moisture for Central America (Durán-Quesada et al., 2010; Lachniet et al., 2007; Maldonado, 2017). The Caribbean Sea is the dominant contributor of moisture, while southern Central America (specifically, Pacific coastal sites in Costa Rica and Panama) also receive moisture originating from the eastern equatorial Pacific in the form of intense convective rainfall when the northeast trade winds are weak. The majority of the moisture that leaves the Pacific is lost over the ocean, so its contributions to the region are low relative to the Caribbean Sea. The trade winds transport moisture directly from the Caribbean Sea over the Caribbean slope and the moisture undergoes orographic uplift and rainout. Consequently, the Caribbean slope experiences a relatively homogeneous precipitation regime and recharge may occur largely below the MCE. On the Pacific slope, air masses become progressively warmer and drier as they advance westward and descend, so that what little moisture remains once the air masses have traversed the mountains can be expected to precipitate and recharge water sources at an elevation higher than the MCE. The orographic effect on MRE can be quantified as simple linear regressions:

$$MRE_P = 1.072\ (MCE) + 45.65 \tag{17a}$$

$$MRE_C = 0.9493\ (MCE) - 28.24 \tag{17b}$$

with coefficients of determination (R^2) = 0.93 (Pacific) and 0.83 (Caribbean), and mean absolute errors (MAEs) = 144 m (Pacific) and 190 m (Caribbean). Including another catchment property (catchment size, minimum catchment elevation, catchment relief) as an additional predictor variable in the models yields improvement in MRE projections but including more than one additional predictor variable beyond MCE does not. Relief was the catchment property that most improved the models:

$$MRE_P = 1.016\ (MCE) + 0.2693\ (relief) - 151.49 \tag{18a}$$

$$MRE_C = 1.110\ (MCE) - 0.1311\ (relief) + 64.25 \tag{18b}$$

with $R^2_{adjusted} = 0.97$, MAE = 97 m (Pacific) and $R^2_{adjusted} = 0.90$, MAE = 137 m (Caribbean). The improvement is greater on the Caribbean slope. Since rainfall is more evenly distributed across the Caribbean slope, catchment properties may play a more substantial role in the determination of MRE than on the Pacific slope, where precipitation is relatively limited to the mountainous interior and decreases westward. This is evident by the general increase of MRE with SWSE on the Caribbean slope, while samples along the Central Pacific coast of Costa Rica (with SWSEs <100 m asl) have some of the highest MREs in the region (> 2000 m asl, Fig. 5). The MRE and MCE relationship was further examined by assessing potential correlations between the MRE:MCE ratio and other catchment properties. The ratio of MRE to MCE trends positively on the Pacific slope but negatively on the Caribbean slope with catchment size,

Table 2
Median MRE from the Pacific domain of Central American countries.

Country	Median Bayesian MRE (m)	Median lapse rate MRE (m)
Costa Rica	1040 ± 272	1979 ± 30
Nicaragua	360 ± 181	1024 ± 15
Honduras	1671 ± 179	1289 ± 27
El Salvador	307 ± 158	1104 ± 119

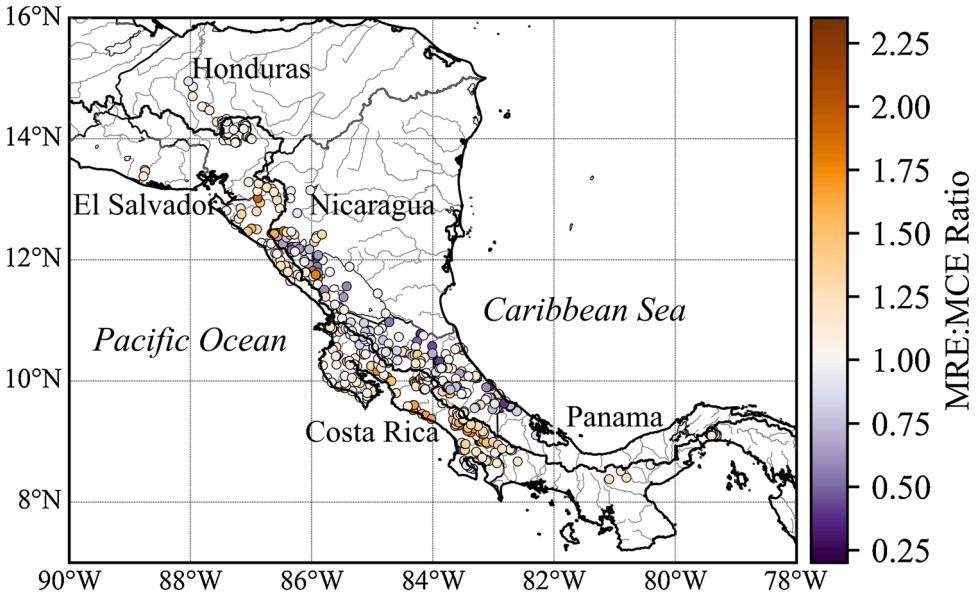

Fig. 10. Map showing the mean recharge elevation (MRE) to mean catchment elevation (MCE) ratio of each surface water site.

SWSE, and relief ($\alpha = 0.05$), suggesting that catchment properties strongly influence the MRE:MCE relationship, likely because these variables are directly related to the MCE ($p < 0.05$ (size) and <0.001 (SWSE, relief for both slopes). In any case, the mechanisms underlying the relationships observed here merit additional consideration beyond this study.

5. Conclusions

This research investigated the utility of implementing isotopic comparisons of surface water samples and interpolated precipitation within a Bayesian framework which considered both the uncertainty in isotopic compositions as well as the potential for evaporative enrichment of the samples to estimate the MRE of water sources in Central America. Bayesian MRE estimates were found to be on average lower than estimates provided by the more simple isoscape approach (Yamanaka and Yamada, 2017) and the traditional isotopic lapse rate method (Sánchez-Murillo et al., 2020), neither of which account for isotopic uncertainties or deviations caused by fractionating phase changes. All isotope-based methods resulted in MREs higher than samples' precipitation-weighted mean catchment elevations (CME_{PW}), which can approximate the actual MRE, but the differences between MRE estimates and CME_{PW} are on average smaller when MREs are estimated using the Bayesian approach. These results demonstrate that the effects of isotopic uncertainty incorporation and evaporative correction in isotope-based MRE determination are significant.

MREs demonstrate a clear difference in patterns of recharge for the Pacific and Caribbean slopes. Surface water sources on the Pacific slope are generally recharged at higher elevations relative to the source MCE, while those on the Caribbean slope are largely recharged at elevations lower than the source MCE. The difference is attributed to the westward direction of moisture transport from the Caribbean Sea, orographic uplift and rainout on the Caribbean slope, and rain shadow on the Pacific slope. The orographic effect on recharge was quantified and can be used to estimate the MRE of other regional water sources based only on knowledge of the source MCE, although including information regarding another catchment property such as catchment size, minimum catchment elevation (SWSE), or catchment relief improves estimations because these variables influence the MRE:MCE relationship. The disparities between MRE and SWSE were higher on the Pacific slope, where most of the region's population is concentrated, confirming the importance of protecting upland areas as critical recharge zones.

While this study revealed meaningful patterns that can contribute to the current understanding of recharge in the Central America region, some factors in the developed approach to MRE estimation had the potential to introduce errors. Interpolation errors associated with the precipitation model are one important factor to consider. Since the most significant model errors are all associated with sites on the Pacific slope (Fig. 4), one possible explanation could be that the model does not directly account for the precipitation amount effect. The amount effect has been identified as a dominant control on isotopic compositions of rainfall in the region, particularly on the Pacific slope of Costa Rica (Sánchez-Murillo and Birkel, 2016) and Panama (Lachniet and Patterson, 2006). Still, the model performed reasonably well with MAEs smaller than those resulting from the global OIPC model (Bowen, 2017; Bowen and Revenaugh, 2003) and similar to those of other regional models over complex terrain (Yamanaka et al., 2015; Yamanaka and Yamada, 2017). Another limitation of this study is the disproportionate distribution of regional data. With the exception of Costa Rica, data from Central American countries is sparse and largely constrained to the Pacific slope. Sampling efforts have historically been concentrated on the Pacific slope according to population distributions but given that the Caribbean Sea is the primary moisture source to the region, isotope data from the Caribbean slope is also relevant (Sánchez-Murillo et al., 2020). In this case, additional Caribbean data would facilitate a more robust comparison between recharge patterns and controls of the two domains. It is therefore reasonable to argue that

further sampling efforts from both domains are needed, as additional data from the Pacific domain could help resolve precipitation model error. Finally, there are a number of other factors beyond evaporation that could potentially affect the isotopic compositions of water sources and should be considered when applying the methods developed here. These include seawater intrusion, especially where coastal aquifers are overdrawn to provide for urban populations (Ballestero et al., 2007; Ferguson and Gleeson, 2012), as well as the large-scale movement of groundwaters (Grasby and Chen, 2005). In this study, samples that were collected within 1 km of coastlines were removed prior to analysis to avoid potential impacts of seawater intrusion.

Overall, the findings of this study have contributed to an enhanced understanding of recharge in Central America. Estimated MREs may be incorporated into GIS-based analyses or runoff or groundwater flow models to chart recharge areas with greater reliability (Yamanaka and Yamada, 2017). Furthermore, these flow models could be coupled with downscaled global climate models to investigate the potential impacts of climate change on the region's water resources (Scibek and Allen, 2006). The quantified MRE-catchment property relationships may be used by governmental institutions to extrapolate the MRE of other water resources in the region, ultimately leading to enhanced water resources management. However, future research should aim to further validate these models when more isotope data, especially from the Caribbean domain, are available. A comparison of Bayesian MRE estimates with recharge-weighted MRE would be informative in this regard, and ET mapping for the determination of recharge-flux may be facilitated via the coupling of process-based models with remote sensing data (Liu et al., 2003). Finally, the higher recharge elevations and larger differences between MRE and SWSE on the Pacific slope (where the majority of the population lives) imply that this information can be used to promote awareness among people of their dependence on mountains for water supply and clarify the importance of establishing protections for the mountainous areas. The methods in the assessment presented here can also be applied to other regions where water isotope data are available or can be obtained and can serve as an example of the effectiveness of using spatial models within a Bayesian probabilistic framework.

Data availability statement

The data that supports the findings of this study are available in the supplementary material of this article.

Funding

Sampling campaigns in Costa Rica, Nicaragua, Honduras, and El Salvador were supported by the International Atomic Energy Agency [grants COS/7/005, RC-19747, and RLA/7/024 to RSM]. Funding from the Research Office of the Universidad Nacional (Heredia, Costa Rica) [grants SIA-0482-13, SIA-0101-14, SIA-0236-16, SIA-411-17, and SIA-414-17] was also crucial for conducting sampling campaigns and stable isotope analysis across the isthmus. In addition, the authors acknowledge the support of the United States National Science Foundation [DEB-1802885].

CRediT authorship contribution statement

L. Nicole Arellano: Investigation, Formal analysis, Writing - original draft, Visualization. **Stephen P. Good:** Conceptualization, Resources, Methodology, Software. **Ricardo Sánchez-Murillo:** Conceptualization, Resources, Funding acquisition, Validation. **W. Todd Jarvis:** Supervision. **David C. Noone:** Resources, Data curation. **Catherine E. Finkenbiner:** Writing - review & editing.

Declaration of Competing Interest

The authors report no declarations of interest.

Acknowledgments

The authors would like to thank Vianeth Reyes-Ibarra, Kaitlyn Mansoorieh, Maxwell Breen, Jake Rose, and Laura Hellmich for their help collecting recent stable isotope samples in Panama.

Appendix A. Supplementary data

Supplementary material related to this article can be found, in the online version, at doi:https://doi.org/10.1016/j.ejrh.2020.100739.

References

Alexander, R.B., Boyer, E.W., Smith, R.A., Schwarz, G.E., Moore, R.B., 2007. The role of headwater streams in downstream water quality. J. Am. Water Resour. Assoc. 43, 41–59. https://doi.org/10.1111/j.1752-1688.2007.00005.x.

Ambach, W., Dansgaard, W., Eisner, H., Møller, J., 1968. The altitude effect on the isotopic composition of precipitation and glacier ice in the Alps. Tellus 20, 595–600. https://doi.org/10.3402/tellusa.v20i4.10040.

Araguás-Araguás, L., Froehlich, K., Rozanski, K., 2000. Deuterium and oxygen-18 isotope composition of precipitation and atmospheric moisture. Hydrol. Process. 14, 1341–1355. https://doi.org/10.1002/1099-1085(20000615)14:8<1341::AID-HYP983>3.0.CO;2-Z.
Ariza, C., Maselli, D., Kohler, T., 2013. Mountains: Our Life, Our Future Progress and Perspectives on Sustainable Mountain Development. Swiss Agency for Development and Cooperation (SDC), Centre for Development and Environment, Bern, Switzerland.
Ballestero, M., Reyes, V., Astorga, Y., 2007. Groundwater in Central America: its importance, development and use, with particular reference to its role in irrigated agriculture. The Agricultural Groundwater Revolution: Opportunities and Threats to Development. CAB International, Wallingford, pp. 100–128. https://doi.org/10.1079/9781845931728.0100.
Bhat, N.A., Jeelani, G., 2015. Delineation of the recharge areas and distinguishing the sources of karst springs in Bringi watershed, Kashmir Himalayas using hydrochemistry and environmental isotopes. J. Earth Syst. Sci. 124, 1667–1676. https://doi.org/10.1007/s12040-015-0629-y.
Bowen, G.J., 2010. Statistical and geostatistical mapping of precipitation water isotope ratios. Isoscapes. Springer, Netherlands, Dordrecht, pp. 139–160. https://doi.org/10.1007/978-90-481-3354-3_7.
Bowen, G.J., 2017. The Online Isotopes in Precipitation Calculator, Version 3.1 [WWW Document]. URL. http://www.waterisotopes.org.
Bowen, G.J., Good, S.P., 2015. Incorporating water isoscapes in hydrological and water resource investigations. Wiley Interdiscip. Rev. Water 2, 107–119. https://doi.org/10.1002/wat2.1069.
Bowen, G.J., Revenaugh, J., 2003. Interpolating the isotopic composition of modern meteoric precipitation. Water Resour. Res. 39 https://doi.org/10.1029/2003WR002086.
Castillo, L.E., de la Cruz, E., Ruepert, C., 1997. Ecotoxicology and pesticides in tropical aquatic ecosystems of Central America. Environ. Toxicol. Chem. 16, 41–51. https://doi.org/10.1002/etc.5620160104.
Clark, I.D., Fritz, P., 1997. Environmental Isotopes in Hydrogeology. CRC Press, New York. https://doi.org/10.1201/9781482242911.
Cosgrove, W.J., Loucks, D.P., 2015. Water management: current and future challenges and research directions. Water Resour. Res. 51, 4823–4839. https://doi.org/10.1002/2014WR016869.
da Costa, A., Salis, H., Viana, J., Pacheco, F., 2019. Groundwater recharge potential for sustainable water use in urban areas of the Jequitiba River Basin, Brazil. Sustainability 11, 2955. https://doi.org/10.3390/su11102955.
Dansgaard, W., 1964. Stable isotopes in precipitation. Tellus 16, 436–468. https://doi.org/10.3402/tellusa.v16i4.8993.
Dehaspe, J., Birkel, C., Tetzlaff, D., Sánchez-Murillo, R., Durán-Quesada, A.M., Soulsby, C., 2018. Spatially distributed tracer-aided modelling to explore water and isotope transport, storage and mixing in a pristine, humid tropical catchment. Hydrol. Process. 32, 3206–3224. https://doi.org/10.1002/hyp.13258.
Diaz, H.F., Grosjean, M., Graumlich, L., 2003. Climate variability and change in high elevation regions: past, present and future. Clim. Change 59, 1–4. https://doi.org/10.1023/A:1024416227887.
Dodds, W.K., Oakes, R.M., 2008. Headwater influences on downstream water quality. Environ. Manage. 41, 367–377. https://doi.org/10.1007/s00267-007-9033-y.
Durán-Quesada, A.M., Gimeno, L., Amador, J.A., Nieto, R., 2010. Moisture sources for Central America: identification of moisture sources using a Lagrangian analysis technique. J. Geophys. Res. 115, D05103 https://doi.org/10.1029/2009JD012455.
Eastoe, C., Towne, D., 2018. Regional zonation of groundwater recharge mechanisms in alluvial basins of Arizona: interpretation of isotope mapping. J. Geochemical Explor. 194, 134–145. https://doi.org/10.1016/j.gexplo.2018.07.013.
Ferguson, G., Gleeson, T., 2012. Vulnerability of coastal aquifers to groundwater use and climate change. Nat. Clim. Change 2, 342–345. https://doi.org/10.1038/nclimate1413.
Fick, S.E., Hijmans, R.J., 2017. WorldClim 2: new 1-km spatial resolution climate surfaces for global land areas. Int. J. Climatol. 37, 4302–4315. https://doi.org/10.1002/joc.5086.
Gat, J.R., Dansgaard, W., 1972. Stable isotope survey of the fresh water occurrences in Israel and the Northern Jordan Rift Valley. J. Hydrol. 16, 177–211. https://doi.org/10.1016/0022-1694(72)90052-2.
Gibson, J.J., Edwards, T.W.D., 2002. Regional water balance trends and evaporation-transpiration partitioning from a stable isotope survey of lakes in northern Canada. Global Biogeochem. Cycles 16, 10-1-10–14. https://doi.org/10.1029/2001GB001839.
Gibson, J.J., Birks, S.J., Edwards, T.W.D., 2008. Global prediction of δ_A and δ 2 H- δ^{18} O evaporation slopes for lakes and soil water accounting for seasonality. Global Biogeochem. Cycles 22. https://doi.org/10.1029/2007GB002997 n/a-n/a.
Gibson, J.J., Birks, S.J., Yi, Y., 2016. Stable isotope mass balance of lakes: a contemporary perspective. Quat. Sci. Rev. 131, 316–328. https://doi.org/10.1016/j.quascirev.2015.04.013.
Gonfiantini, R., Roche, M.-A., Olivry, J.-C., Fontes, J.-C., Zuppi, G.M., 2001. The altitude effect on the isotopic composition of tropical rains. Chem. Geol. 181, 147–167. https://doi.org/10.1016/S0009-2541(01)00279-0.
Good, S.P., Kennedy, C.D., Stalker, J.C., Chesson, L.A., Valenzuela, L.O., Beasley, M.M., Ehleringer, J.R., Bowen, G.J., 2014. Patterns of local and nonlocal water resource use across the western U.S. determined via stable isotope intercomparisons. Water Resour. Res. 50, 8034–8049. https://doi.org/10.1002/2014WR015884.
Grasby, S.E., Chen, Z., 2005. Subglacial recharge into the Western Canada Sedimentary Basin—impact of Pleistocene glaciation on basin hydrodynamics. Geol. Soc. Am. Bull. 117, 500. https://doi.org/10.1130/B25571.1.
Gunawardhana, L.N., Al-Rawas, G.A., Kazama, S., 2017. An alternative method for predicting relative humidity for climate change studies. Meteorol. Appl. 24, 551–559. https://doi.org/10.1002/met.1641.
Guo, X., Tian, L., Wang, L., Yu, W., Qu, D., 2017. River recharge sources and the partitioning of catchment evapotranspiration fluxes as revealed by stable isotope signals in a typical high-elevation arid catchment. J. Hydrol. 549, 616–630.
Hall, B., Currell, M., Webb, J., 2020. Using multiple lines of evidence to map groundwater recharge in a rapidly urbanising catchment: implications for future land and water management. J. Hydrol. 580, 124265 https://doi.org/10.1016/j.jhydrol.2019.124265.
IAEA, 2014. IAEA/GNIP Precipitation Sampling Guide Introduction: the Global Network of Isotopes in Precipitation (GNIP).
IAEA/WMO, 2015. Global Network of Isotopes in Precipitation [WWW Document]. GNIP Database. URL. https://nucleus.iaea.org/wiser.
Imbach, P., Chou, S.C., Lyra, A., Rodrigues, D., Rodriguez, D., Latinovic, D., Siqueira, G., Silva, A., Garofolo, L., Georgiou, S., 2018. Future climate change scenarios in Central America at high spatial resolution. PLoS One 13 e0193570.
Jasechko, S., Taylor, R.G., 2015. Intensive rainfall recharges tropical groundwaters. Environ. Res. Lett. 10, 124015 https://doi.org/10.1088/1748-9326/10/12/124015.
Jeelani, G., Shah, R.A., Deshpande, R.D., 2018. Application of water isotopes to identify the sources of groundwater recharge in a karstified landscape of Western Himalaya. J. Clim. Change 4, 37–47. https://doi.org/10.3233/JCC-180005.
Jung, Y.-Y., Koh, D.-C., Yoon, Y.-Y., Kwon, H.-I., Heo, J., Ha, K., Yun, S.-T., 2019. Using stable isotopes and tritium to delineate groundwater flow systems and their relationship to streams in the Geum River basin, Korea. J. Hydrol. 573, 267–280. https://doi.org/10.1016/J.JHYDROL.2019.03.084.
Karim, A., Veizer, J., 2002. Water balance of the Indus River Basin and moisture source in the Karakoram and western Himalayas: implications from hydrogen and oxygen isotopes in river water. J. Geophys. Res. Atmos. 107 https://doi.org/10.1029/2000JD000253. ACH 9-1-ACH 9-12.
Kennedy, C.D., Bowen, G.J., Ehleringer, J.R., 2011. Temporal variation of oxygen isotope ratios (δ18O) in drinking water: Implications for specifying location of origin with human scalp hair. Forensic Sci. Int. 208, 156–166. https://doi.org/10.1016/J.FORSCIINT.2010.11.021.
Koeniger, P., Toll, M., Himmelsbach, T., 2016. Stable isotopes of precipitation and spring waters reveal an altitude effect in the Anti-Lebanon Mountains, Syria. Hydrol. Process. 30, 2851–2860. https://doi.org/10.1002/hyp.10822.
Koeniger, P., Margane, A., Abi-Rizk, J., Himmelsbach, T., 2017. Stable isotope-based mean catchment altitudes of springs in the Lebanon Mountains. Hydrol. Process. 31, 3708–3718. https://doi.org/10.1002/hyp.11291.
Křeček, J., Haigh, M.J., 2000. Reviewing the contexts of headwater control. Environmental Reconstruction in Headwater Areas. Springer, Netherlands, Dordrecht, pp. 9–24. https://doi.org/10.1007/978-94-011-4134-5_2.
Křeček, J., Haigh, M., 2019. Land use policy in headwater catchments. Land Use Policy 80, 410–414. https://doi.org/10.1016/J.LANDUSEPOL.2018.03.043.

Lachniet, M.S., Patterson, W.P., 2006. Use of correlation and stepwise regression to evaluate physical controls on the stable isotope values of Panamanian rain and surface waters. J. Hydrol. 324, 115–140. https://doi.org/10.1016/j.jhydrol.2005.09.018.
Lachniet, M.S., Patterson, W.P., 2009. Oxygen isotope values of precipitation and surface waters in northern Central America (Belize and Guatemala) are dominated by temperature and amount effects. Earth Planet. Sci. Lett. 284, 435–446. https://doi.org/10.1016/j.epsl.2009.05.010.
Lachniet, M.S., Patterson, W.P., Burns, S., Asmerom, Y., Polyak, V., 2007. Caribbean and Pacific moisture sources on the Isthmus of Panama revealed from stalagmite and surface water δ 18 O gradients. Geophys. Res. Lett. 34, L01708 https://doi.org/10.1029/2006GL028469.
Lehner, B., Verdin, K., Jarvis, A., 2008. New Global Hydrography Derived From Spaceborne Elevation Data, Eos Transactions. AGU. https://doi.org/10.1029/2008EO100001.
Lentswe, G.B., Molwalefhe, L., 2020. Delineation of potential groundwater recharge zones using analytic hierarchy process-guided GIS in the semi-arid Motloutse watershed, eastern Botswana. J. Hydrol. Reg. Stud. 28, 100674 https://doi.org/10.1016/j.ejrh.2020.100674.
Leonard, H.J., 1987. Natural Resources and Economic Development in Central America. Transaction Books, New Brunswick, NJ.
Liu, J., Chen, J.M., Cihlar, J., 2003. Mapping evapotranspiration based on remote sensing: an application to Canada's landmass. Water Resour. Res. 39 https://doi.org/10.1029/2002WR001680.
Longinelli, A., Selmo, E., 2003. Isotopic composition of precipitation in Italy: a first overall map. J. Hydrol. 270, 75–88. https://doi.org/10.1016/S0022-1694(02)00281-0.
Magaña, V., Amador, J.A., Medina, S., 1999. The midsummer drought over Mexico and Central America. J. Clim. 12, 1577–1588. https://doi.org/10.1175/1520-0442(1999)012<1577:TMDOMA>2.0.CO;2.
Maldonado, T., 2017. The early rainy season in Central America: the role of the tropical North Atlantic SSTs. Int. J. Climatol.
Maldonado, T., Alfaro, E., Fallas-López, B., Alvarado, L., 2013. Seasonal prediction of extreme precipitation events and frequency of rainy days over Costa Rica, Central America, using canonical correlation analysis. Adv. Geosci. 33, 41–52. https://doi.org/10.5194/adgeo-33-41-2013.
Maria, A., Acero, J.L., Aguilera, A.I., Lozano, M.G., 2017. Central America Urbanization Review Making Cities Work for Central America Directions in Development Countries and Regions. Washington, DC. https://doi.org/10.1596/978-1-4648-0985-9.
Matiatos, I., Alexopoulos, A., 2011. Application of stable isotopes and hydrochemical analysis in groundwater aquifers of Argolis Peninsula (Greece). Isotopes Environ. Health Stud. 47, 512–529. https://doi.org/10.1080/10256016.2011.617883.
Maurer, E.P., Roby, N., Stewart-Frey, I.T., Bacon, C.M., 2017. Projected twenty-first-century changes in the Central American mid-summer drought using statistically downscaled climate projections. Reg. Environ. Change 17, 2421–2432. https://doi.org/10.1007/s10113-017-1177-6.
Meredith, K., Cendón, D., Pigois, J.-P., Hollins, S., Jacobsen, G., 2011. Using C-14 and H-3 to delineate a recharge "window" into the Perth Basin aquifers, North Gnangara groundwater system, Western Australia. Sci. Total Environ. 414, 456–469. https://doi.org/10.1016/j.scitotenv.2011.10.016.
Mosase, E., Ahiablame, L., Park, S., Bailey, R., 2019. Modelling potential groundwater recharge in the Limpopo River Basin with SWAT-MODFLOW. Groundw. Sustain. Dev. 9, 100260 https://doi.org/10.1016/j.gsd.2019.100260.
O'Driscoll, M.A., DeWalle, D.R., McGuire, K.J., Gburek, W.J., 2005. Seasonal 18O variations and groundwater recharge for three landscape types in central Pennsylvania, USA. J. Hydrol. 303, 108–124. https://doi.org/10.1016/j.jhydrol.2004.08.020.
Parello, F., Aiuppa, A., Calderon, H., Calvi, F., Cellura, D., Martinez, V., Militello, M., Vammen, K., Vinti, D., 2008. Geochemical characterization of surface waters and groundwater resources in the Managua area (Nicaragua, Central America). Appl. Geochem. 23, 914–931. https://doi.org/10.1016/j.apgeochem.2007.08.006.
Paternoster, M., Liotta, M., Favara, R., 2008. Stable isotope ratios in meteoric recharge and groundwater at Mt. Vulture volcano, southern Italy. J. Hydrol. 348, 87–97. https://doi.org/10.1016/J.JHYDROL.2007.09.038.
Perez, J., Silva, A., Inguaggiato, S., Ortega, M., Pérez, J., Heilweil, V., 2015. Meteoric isotopic gradient on the windward side of theSierra Madre Oriental area, Veracruz – mexico. Geofis. Int. 54, 267–276. https://doi.org/10.1016/j.gi.2015.04.021.
Pourghasemi, H.R., Sadhasivam, N., Yousefi, S., Tavangar, S., Ghaffari Nazarlou, H., Santosh, M., 2020. Using machine learning algorithms to map the groundwater recharge potential zones. J. Environ. Manage. 265, 110525 https://doi.org/10.1016/j.jenvman.2020.110525.
Putman, A.L., Fiorella, R.P., Bowen, G.J., Cai, Z., 2019. A global perspective on local meteoric water lines: meta-analytic insight into fundamental controls and practical constraints. Water Resour. Res. 55, 6896–6910. https://doi.org/10.1029/2019WR025181.
Sáenz, F., Durán-Quesada, A.M., 2015. A climatology of low level wind regimes over Central America using a weather type classification approach. Front. Earth Sci. 3, 15. https://doi.org/10.3389/feart.2015.00015.
Sánchez-Murillo, R., Birkel, C., 2016. Groundwater recharge mechanisms inferred from isoscapes in a complex tropical mountainous region. Geophys. Res. Lett. 43, 5060–5069. https://doi.org/10.1002/2016GL068888.
Sánchez-Murillo, R., Esquivel Hernández, G., Welsh, K., Brooks, E., Boll, J., Solís, R., Valdés, J., 2013. Spatial and temporal variation of stable isotopes in precipitation across Costa rica: an analysis of historic GNIP records. Open J. Mod. Hydrol. 3, 226–240. https://doi.org/10.4236/ojmh.2013.34027.
Sánchez-Murillo, R., Esquivel-Hernández, G., Sáenz-Rosales, O., Piedra-Marín, G., Fonseca-Sánchez, A., Madrigal-Solís, H., Ulloa-Chaverri, F., Rojas-Jiménez, L.D., Vargas-Víquez, J.A., 2016. Isotopic composition in precipitation and groundwater in the northern mountainous region of the Central Valley of Costa rica. Isotopes Environ. Health Stud. 53, 1–17. https://doi.org/10.1080/10256016.2016.1193503.
Sánchez-Murillo, R., Esquivel-Hernández, G., Corrales-Salazar, J.L., Castro-Chacón, L., Durán-Quesada, A.M., Guerrero-Hernández, M., Delgado, V., Barberena, J., Montenegro-Rayo, K., Calderón, H., Chevez, C., Peña-Paz, T., García-Santos, S., Ortiz-Roque, P., Alvarado-Callejas, Y., Benegas, L., Hernández-Antonio, A., Matamoros-Ortega, M., Ortega, L., Terzer-Wassmuth, S., 2020. Tracer hydrology of the data-scarce and heterogeneous Central American Isthmus. Hydrol. Process. 34, 2660–2675. https://doi.org/10.1002/hyp.13758.
Sappa, G., Vitale, S., Ferranti, F., 2018. Identifying karst aquifer recharge areas using environmental isotopes: a case study in central italy. Geosciences 8, 351. https://doi.org/10.3390/geosciences8090351.
SaravanaKumar, U., Kumar, B., Rai, S.P., Sharma, S., 2010. Stable isotope ratios in precipitation and their relationship with meteorological conditions in the Kumaon Himalayas, India. J. Hydrol. 391, 1–8. https://doi.org/10.1016/j.jhydrol.2010.06.019.
Saylor, J.E., Mora, A., Horton, B.K., Nie, J., 2009. Controls on the isotopic composition of surface water and precipitation in the Northern Andes, Colombian Eastern Cordillera. Geochim. Cosmochim. Acta 73, 6999–7018. https://doi.org/10.1016/j.gca.2009.08.030.
Scibek, J., Allen, D.M., 2006. Modeled impacts of predicted climate change on recharge and groundwater levels. Water Resour. Res. 42. https://doi.org/10.1029/2005WR004742.
Siegenthaler, U., Oeschger, H., 1980. Correlation of 18O in precipitation with temperature and altitude. Nature 285, 314–317. https://doi.org/10.1038/285314a0.
Silva, A.H., Carcaño, M., Lopez, L., Morán, C., Perales, J.M., 2015. Microbial contamination of water in Laguna de Metapan Elsalvador, Central America. Toxicol. Lett. 238, S90. https://doi.org/10.1016/j.toxlet.2015.08.302.
Spehn, M.E., Rudmann-Maurer, K., Korner, C., 2010. Mountain Biodiversity and Global Change. Swiss Agency for Development and Cooperation (SDS), GMBA-DIVERSITAS, Basel.
Sprenger, M., Tetzlaff, D., Soulsby, C., 2017. Soil water stable isotopes reveal evaporation dynamics at the soil–plant–atmosphere interface of the critical zone. Hydrol. Earth Syst. Sci. Discuss. 21, 3839–3858. https://doi.org/10.5194/hess-21-3839-2017.
Taylor, M.A., Alfaro, E.J., 2005. Climate of Central America and the Caribbean. Encyclopedia of World Climatology. Springer, Netherlands, pp. 183–189. https://doi.org/10.1007/1-4020-3266-8_37.
Taylor, R.G., Scanlon, B., Döll, P., Rodell, M., van Beek, R., Wada, Y., Longuevergne, L., Leblanc, M., Famiglietti, J.S., Edmunds, M., Konikow, L., Green, T.R., Chen, J., Taniguchi, M., Bierkens, M.F.P., MacDonald, A., Fan, Y., Maxwell, R.M., Yechieli, Y., Gurdak, J.J., Allen, D.M., Shamsudduha, M., Hiscock, K., Yeh, P.J.-F., Holman, I., Treidel, H., 2012. Ground water and climate change. Nat. Clim. Change 3, 322.
Tetzlaff, D., Soulsby, C., Waldron, S., Malcolm, I.A., Bacon, P.J., Dunn, S.M., Lilly, A., Youngson, A.F., 2007. Conceptualization of runoff processes using a geographical information system and tracers in a nested mesoscale catchment. Hydrol. Process. 21, 1289–1307. https://doi.org/10.1002/hyp.6309.
Vespasiano, G., Apollaro, C., De Rosa, R., Muto, F., Larosa, S., Fiebig, J., Mulch, A., Marini, L., 2015. The Small Spring Method (SSM) for the definition of stable isotope–elevation relationships in Northern Calabria (Southern Italy). Appl. Geochem. 63, 333–346. https://doi.org/10.1016/j.apgeochem.2015.10.001.

Villegas, P., Paredes, V., Betancur, T., Taupin, J.D., Toro, L.E., 2018. Groundwater evolution and mean water age inferred from hydrochemical and isotopic tracers in a tropical confined aquifer. Hydrol. Process. 32, 2158–2175. https://doi.org/10.1002/HYP.13160.

Viviroli, D., Weingartner, R., 2004. The hydrological significance of mountains: from regional to global scale. Hydrol. Earth Syst. Sci.

Wassenaar, L., Van Wilgenburg, S., Larson, K., Hobson, K., 2009. A groundwater isoscape (δ D,δ18O) for Mexico. J. Geochemical Explor. 102, 167–174. https://doi.org/10.1016/j.gexplo.2009.01.001.

Winckel, A., Marlin, C., Dever, L., Morel, J.-L., Morabiti, K., Makhlouf, M.B., Chalouan, A., 2002. Apport des isotopes stables dans l'estimation des altitudes de recharge de sources thermales du Maroc. Comptes Rendus Geosci. 334, 469–474. https://doi.org/10.1016/S1631-0713(02)01764-9.

Yamanaka, T., Yamada, Y., 2017. Regional assessment of recharge elevation of tap water sources using the isoscape approach. Res. Dev. 37, 198–205. https://doi.org/10.1659/MRD-JOURNAL-D-16-00066.1.

Yamanaka, T., Makino, Y., Wakiyama, Y., Kishi, K., Maruyama, K., Kano, M., Ma, W., Suzuki, K., 2015. How reliable are modeled precipitation isoscapes over a high-relief mountainous region? Hydrol. Res. Lett. 9, 118–124. https://doi.org/10.3178/hrl.9.118.

Zhu, L., Fan, M., Hough, B., Li, L., 2018. Spatiotemporal distribution of river water stable isotope compositions and variability of lapse rate in the central Rocky Mountains: controlling factors and implications for paleoelevation reconstruction. Earth Planet. Sci. Lett. 496, 215–226. https://doi.org/10.1016/j.epsl.2018.05.047.